ISSN 0023-1584, Kinetics and Catalysis, 2009, Vol. 50, No. 2, pp. 205–219. © Pleiades Publishing, Ltd., 2009.
Original Russian Text © L.I. Kuznetsova, L.G. Detusheva, N.I. Kuznetsova, S.V. Koshcheev, V.I. Zaikovskii, Yu.A. Chesalov, V.A. Rogov, V.B. Fenelonov, V.A. Likholobov, 2009, published in Kinetika i Kataliz, 2009, Vol. 50, No. 2, pp. 218–232.

Catalytic Properties of Platinum-Promoted Acid Cesium Salts of Molybdophosphoric and Molybdovanadophosphoric Heteropoly Acids in the Gas-Phase Oxidation of Benzene to Phenol with an $O_2 + H_2$ Mixture

L. I. Kuznetsova[a], L. G. Detusheva[a], N. I. Kuznetsova[a], S. V. Koshcheev[a], V. I. Zaikovskii[a], Yu. A. Chesalov[a], V. A. Rogov[a], V. B. Fenelonov[a], and V. A. Likholobov[b]

[a] *Boreskov Institute of Catalysis, Siberian Branch, Russian Academy of Sciences, Novosibirsk, 630090 Russia*
e-mail: livkuzn@catalysis.nsk.su

[b] *Institute of Hydrocarbon Processing, Siberian Branch, Russian Academy of Sciences, Omsk, 644040 Russia*

Received April 4, 2007

Abstract—Acid salts $Cs_xH_{3+n-x}PMo_{12-n}V_nO_{40}$ (n = 0, 1, 2, or 3; x = 2.5 or 3.5) with coprecipitated or supported platinum were studied using thermogravimetry, IR spectroscopy, and temperature-programmed reduction. The thermal region of the full stability of these salts is limited by the decomposition temperature of the corresponding acid $H_3PMo_{12}O_{40}$ (~400°C) or $H_{3+n}PMo_{12-n}V_nO_{40}$ (~300–350°C). The degree of reduction of heteropoly anions with hydrogen is regulated by temperature. Deeply reduced heteropoly anions (at 300°C) are slowly oxidized with oxygen with structure and composition regeneration. The states of molybdenum and vanadium on the surface of samples with coprecipitated platinum $Pt_{0.1}$-$Cs_{2.5}H_{0.5}PMo_{12}O_{40}$ (**1**) and $Pt_{0.1}$-$Cs_{2.5}H_{2.5}PMo_{10}V_2O_{40}$ (**2**), which were studied using XPS, correspond to reduced or reoxidized heteropoly anions in the bulk. Platinum metal particles of ~5 nm in size were observed in high-resolution TEM images obtained after the reduction and storage of sample **1** in air. A heteropoly compound forms two texture levels: spherical nanoparticles of 10–20 nm in size are collected in closely packed globules of 100–300 nm in size. Detailed texture studies, which were performed using nitrogen adsorption isotherms, demonstrated texture mobility under the ambient conditions. The cesium salts of the heteropoly acids were tested in the gas-phase oxidation of benzene to phenol with an $O_2 + H_2$ mixture at 180°C. The effect of platinum concentration on the specific catalytic activity in the presence of deeply reduced heteropoly anions was monitored. The samples containing the salt $Cs_{2.5}H_{0.5}PMo_{12}O_{40}$ exhibited the highest activity in the formation of phenol. The introduction of vanadium into the heteropoly anion impaired the catalytic performance of both deeply and slightly reduced samples.

DOI: 10.1134/S0023158409020104

INTRODUCTION

A great number of publications, for example, those surveyed in reviews [1, 2], have been devoted to studies of the cesium salts of heteropoly acids (HPAs) as catalysts for the gas-phase conversions of organic compounds. Insoluble Cs salts are prepared as porous precipitates with a large specific surface area (S_{BET} = 100–200 m^2/g); the elemental composition of the salts can be varied. These properties allow one to design catalysts for various reactions based on the cesium salts of HPAs. The salts $Cs_xH_{3-x}PW_{12}O_{40}$ are the most perfectly studied catalysts for acid–base reactions [1–4]. According to current concepts [1], catalysis with the participation of protons either occurs on the surface of solid acid salts of HPAs (surface type) or in the bulk of the solid acid salts (pseudoliquid bulk type I). On bifunctional catalysts containing $Cs_xH_{3-x}PW_{12}O_{40}$ and metals (Pt, Pd, or Rh), the reactions of *n*-alkane isomerization [1, 2], hydrocarbon oxidation [1, 5], and dimethyl ether carbonylation [3, 4] can be performed using one of the above modes. A more complicated question concerns the zone in which oxidation reactions are catalyzed by molybdovanadophosphoric heteropoly compounds, which are characterized by a change in the oxidation states of molybdenum and vanadium. The reactions can occur on the surface but with the participation of the bulk of the catalyst because of the high proton and electron conductivity of HPAs (bulk catalysis, type II) [1].

The catalytic properties of the acid salts $Cs_xH_{3-x}PMo_{12}O_{40}$ and $Cs_xH_{3+n-x}PMo_{12-n}V_nO_{40}$ in oxidation reactions are less well understood. As examples, the salts $Cs_{2.5}H_{0.5+n}PMo_{12-n}V_nO_{40}$, which mediated the gas-phase oxidation (350°C) of isobutyric acid to methacrylic acid [6], can be mentioned. The thermal instability of heteropoly compounds under catalytic reaction conditions was noted. Another example is the oxidation of light alkanes (isobutane, propane, and ethane) with the use of the acid salts $Cs_xH_{3-x}PMo_{12}O_{40}$ and

$Cs_{2.5}H_{1.5}PMo_{11}V_1O_{40}$, either individually or in the presence of added redox-active ions Fe^{3+}, Ni^{2+}, Mn^{2+}, Cu^{2+}, Co^{2+}, etc. [7–9]. The reactions were performed at high temperatures (340–425°C) to reach a higher yield of valuable products. In view of the thermal instability of the heteropoly compounds [6], the catalytic properties in the above examples are due to mixed oxide compounds formed from heteropoly compounds rather than to the parent heteropoly compounds [7].

The oxidation of methane to formic acid with an $O_2 + H_2$ mixture using $Cs_{2.5}H_{0.5+n}PMo_{12-n}V_nO_{40}$ with platinum group metal ion admixtures was performed at a lower temperature (200–300°C) [10]. In this reaction, the stability of the heteropoly compound was also crucial. In the sample of $Pd_{0.08}Cs_{2.5}H_{1.34}PMo_{11}VO_{40}$, vanadium left the composition of the heteropoly anion as a result of catalytic tests at 300°C, as judged from changes in the shape of the absorption band ν(P–O) at 1060 cm^{-1} in the IR spectra.

In addition to thermal stability, structural changes up to heteropoly anion decomposition can occur under reaction conditions (reducing atmosphere) with HPAs or their salts. These changes are associated with the loss of oxygen atoms because of the reduction of heteropoly anions [11]. The products, such as water, which is formed in the gas-phase oxidation of benzene to phenol with an $O_2 + H_2$ mixture at 180°C in the presence of platinum and molybdophosphoric HPAs, can change the state of heteropoly compounds [12–14].

The aim of this work was to determine the states of components in Pt-$Cs_xH_{3+n-x}PMo_{12-n}V_nO_{40}$ catalysts containing coprecipitated platinum or Pt/$Cs_xH_{3+n-x}PMo_{12-n}V_nO_{40}$ with supported platinum (n = 0, 1, 2, or 3; x = 2.5 or 3.5), both initial and after the reductive treatment with hydrogen, and in the gas-phase oxidation of benzene with an $O_2 + H_2$ mixture. The properties of this system were considered at the following three structural levels [1]: the primary Keggin structure of heteropoly anions; the distribution of H^+ and Cs^+ counterions and platinum between heteropoly anions in the catalysts; and the accessible specific surface area and pore structure, which depend on the aggregation of the primary particles of the heteropoly compound.

EXPERIMENTAL

Preparation of Heteropoly Compounds and Catalysts

The HPA $H_3PMo_{12}O_{40}$ was prepared by the purification of the HPA reagent of analytical grade using ether extraction. The solutions of the HPA $H_{3+n}PMo_{12-n}V_nO_{40}$ (n = 1, 2, or 3) were prepared in accordance with a published procedure [15]. The acid salts $Cs_xH_{3+n-x}PMo_{12-n}V_nO_{40} \cdot mH_2O$ (n = 0, 1, 2, or 3) were prepared by adding an aqueous solution of CsOH (8 ml; 0.25 or 0.35 M for x = 2.5 or 3.5, respectively) to the solutions of corresponding HPAs (10 ml; 0.08 M) at room temperature. The samples were evaporated to dryness at 60°C.

In the preparation of the platinum-containing salts $Pt_{0.1}$-$Cs_{2.5}H_{0.5+n}PMo_{12-n}V_nO_{40} \cdot mH_2O$ (n = 0, 1, 2, or 3) by coprecipitation, an aqueous solution of $Pt(NH_3)_4Cl_2$ was added to the solutions of corresponding HPAs in the molar ratio Pt/HPA = 0.1 followed by the addition of a titrated solution of CsOH in the molar ratio Cs/HPA = 2.5. The samples were evaporated and dried at 60°C. The IR spectra of $Pt_{0.1}$-$Cs_{2.5}H_{0.5}PMo_{12}O_{40} \cdot mH_2O$ contained absorption bands at 1063, 964, 867, and 791 cm^{-1}; the IR spectra of $Pt_{0.1}$-$Cs_{2.5}H_{0.5+n}PMo_{12-n}V_nO_{40} \cdot mH_2O$ (n = 1, 2, or 3) contained absorption bands at 1060–1056, 963, 864, and 790–785 cm^{-1} (Fig. 1, spectra *1–4*).

The supported catalysts $Pt_{0.1}/Cs_xH_{3+n-x}PMo_{12-n}V_nO_{40} \cdot mH_2O$ (n = 0, 1, 2, or 3; x = 2.5 or 3.5) were prepared by impregnating acid cesium salts with a solution of H_2PtCl_6 taken in a ratio of Pt : HPA = 0.1. The samples were dried at 60°C. The IR spectra contained the following absorption bands: $Pt_{0.1}/Cs_{2.5}H_{0.5}PMo_{12}O_{40} \cdot mH_2O$, 1062, 963, 865, and 785 cm^{-1}; $Pt_{0.1}/Cs_{2.5}H_{0.5+n}PMo_{12-n}V_nO_{40} \cdot mH_2O$ (n = 1, 2, or 3), 1060–1055, 960–955, 865–858, and 780–770 cm^{-1}; and $Pt_{0.1}/Cs_{3.5}H_{n-0.5}PMo_{12-n}V_nO_{40} \cdot mH_2O$ (n = 1, 2, or 3), 1065–1060, 965–962, 860, and 785 cm^{-1}.

The catalysts were reduced in a flow of hydrogen at 300 or 200°C for 1 h.

IR spectroscopy. The IR spectra of the samples were recorded on a Bomem M-102 FTIR spectrometer over the spectral range of 2000–250 cm^{-1}; the resolution was 4 cm^{-1}. Before the measurement of the IR spectra, the samples were pelletized with KBr (a portion of 2 mg per 500 mg of KBr). The deconvolution of absorption bands into individual Gaussian components was performed using the Microcal Origin V. 6.0 program.

Thermogravimetric analysis. The thermogravimetric analysis of cesium salts was performed on a Q-1500 D derivatograph (Paulik–Paulik–Erdey) in a flow of helium (25 l/h) at a heating rate of 5 K/min from room temperature to 600°C. The sample weight was 200 mg (or 1000 mg); the accuracy of measurements was ±0.3 mg.

Temperature-programmed reduction (TPR). The TPR was performed in a flow system with a thermal-conductivity detector. Before reduction, the sample was conditioned in O_2 at 300°C for 0.5 h, cooled to room temperature in O_2, and purged with argon. The sample weight was 100 mg; the flow rate of the reducing mixture (10% H_2 in Ar) was 40 cm^3/min, and the heating rate was 10 K/min.

X-ray photoelectron spectroscopy (XPS). XPS spectra were measured using an ES-300 instrument (Kratos Analytical). The samples were applied to a

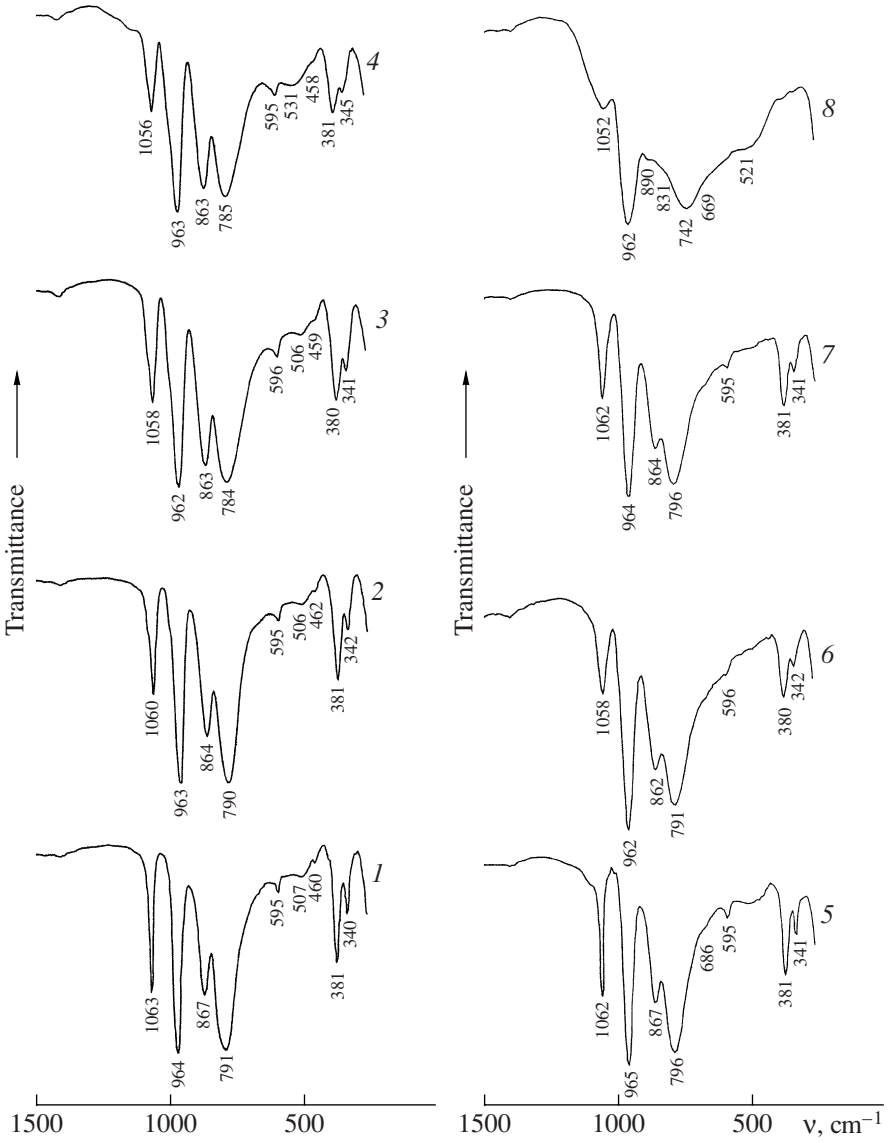

Fig. 1. IR spectra of the initial samples of (*1*–*4*) of acid cesium salts of HPAs coprecipitated with platinum and (*5*–*8*) the same compounds after reduction with H_2 at 200°C and catalytic reaction: *1*, *5*, $Pt_{0.1}$-$Cs_{2.5}H_{0.5}PMo_{12}O_{40} \cdot 3.8H_2O$; *2*, *6*, $Pt_{0.1}$-$Cs_{2.5}H_{1.5}PMo_{11}VO_{40} \cdot 4.7H_2O$; *3*, *7*, $Pt_{0.1}$-$Cs_{2.5}H_{2.5}PMo_{10}V_2O_{40} \cdot 5.4H_2O$; and *4*, *8*, $Pt_{0.1}$-$Cs_{2.5}H_{3.5}PMo_9V_3O_{40} \cdot 6.0H_2O$.

holder using a conducting two-sided adhesive tape. The spectra were measured in a vacuum at room temperature with the excitation of photoelectrons by MgK_α radiation ($h\nu$ = 1253.6 eV) from an anticathode filtered with an Al window. The determination of element concentrations and the line shape analysis with deconvolution into individual components were performed as described elsewhere [14]. The binding energies of peaks were corrected for sample charging using the C 1*s* line (284.8 eV).

High-resolution transmission electron microscopy (HRTEM). The HRTEM images were obtained using a JEM-2010 instrument with a grid resolution of 0.14 nm and an accelerating voltage of 200 kV. The samples were prepared from a powder suspension in hexane by deposition onto a porous carbon substrate fixed on copper gauze.

Adsorption studies. The isotherms of N_2 adsorption at –196°C were measured using an ASAP-2400 instrument after training the samples in a vacuum at 150°C. These isotherms were used to calculate the total accessible surface area by the BET method (S_{BET}), the total pore volume V_Σ with effective sizes to 100–200 nm (from the adsorption at a relative nitrogen pressure of ~0.99), the characteristic mesopore size distribution (from the desorption branch of an isotherm using the BJH method [16]), the micropore volume V_μ, and the mesopore surface area S_α remaining

Table 1. Thermogravimetric analysis of the acid cesium salts of HPAs

No.	Composition	$T_{1,\max}$, °C (m, H_2O/heteropoly anion)	$T_{2,\max}$, °C	$T_{3,\max}$, °C	ΔT, °C (q, H_2O/heteropoly anion)
1	$Cs_{2.5}H_{0.5}PMo_{12}O_{40} \cdot mH_2O + 0.1H_2PtCl_6$	135(4.7)	–	–	–
2	$Cs_{2.5}H_{0.5}PMo_{12}O_{40} \cdot mH_2O + 0.1Pt(NH_3)_4Cl_2$	135(7.9)	230; ~400	–	–
3	$Cs_{2.5}H_{0.5}PMo_{12}O_{40} \cdot mH_2O$*	155(3.8)	415; 440	**	280–600 (0.17)
4	$Cs_{2.5}H_{1.5}PMo_{11}VO_{40} \cdot mH_2O$	150(4.7)	~300	490, *exo***	210–500 (0.49)
5	$Cs_{2.5}H_{2.5}PMo_{10}V_2O_{40} \cdot mH_2O$	150(5.4)	~350	570, *endo*	250–500 (0.60)
6	$Cs_{2.5}H_{3.5}PMo_9V_3O_{40} \cdot mH_2O$	150(6.0)	280	540, *endo*	230–500 (0.89)
7	$Cs_{3.5}H_{2.5}PMo_9V_3O_{40} \cdot mH_2O$	155(5.5)	–	**	230–460 (1.0)

* Sample weight of 1000 mg; for the other samples, 200 mg.
** Weakly pronounced features.

after the filling of micropores (using a comparative method [16, 17]).

True density. The true density of the cesium salt was measured using an Autopycnometer 1340 instrument using helium.

Catalytic measurements. The catalytic measurements were performed in a flow reactor with the inner circulation of the gas phase (the so-called Berty reactor). The inlet flow rates of O_2, H_2, and N_2 were set using mass flow controllers; benzene was supplied using a syringe-type pump. The flow rates were 10, 5, 8, and 85 or 20, 10, 8, and 178 ml/min for H_2, O_2, C_6H_6, and N_2, respectively. The reaction temperature was 180°C; the catalyst powder weight was 0.3 or 0.1 g. The unit was equipped with a system for the GC analysis of gases at the reactor outlet.

RESULTS AND DISCUSSION

Composition and Thermal Stability of Acid Cesium Salts

The cesium HPA salts $Cs_xH_{3+n-x}PMo_{12-n}V_nO_{40} \cdot mH_2O$ (n = 0, 1, 2, or 3) were promoted with platinum in a molar ratio of Pt/HPA = 0.1. The IR spectra of the resulting samples included a set of bands in the region of 1100–600 cm^{-1} (Fig. 1, spectra *1–4*; see also Experimental), which is characteristic of the Keggin structure $PMo_{12}O_{40}^{3-}$ or $PMo_{12-n}V_nO_{40}^{(3+n)-}$ heteropoly anions [18, 9]. As can be seen in Fig. 1, the structure of the heteropoly anion was unchanged upon the replacement of protons in the heteropoly anion by Cs^+ followed by the introduction of Pt(II) by coprecipitation or impregnation. The spectra of the samples containing acid Cs salts of the anions $PMo_{12-n}V_nO_{40}^{(3+n)-}$ differ from the spectra of the samples containing the acid Cs salt of the anion $PMo_{12}O_{40}^{3-}$ in that the absorption band at 1060 cm^{-1} (P–O) is weakly split and the absorption band at 790–785 cm^{-1} (Mo–O_s–Mo (or V), where O_s is the structural oxygen) is broadened because of a structure distortion upon the substitution of vanadium(V) for Mo(VI) ions.

Table 1 summarizes the results of the thermogravimetric analysis of Pt-containing samples and the corresponding acid cesium salts. Clearly pronounced endotherms with a maximum at T_1 = 135–155°C accompanied by weight loss were observed on heating the samples of the acid cesium salts of HPAs under dynamic conditions (Fig. 2). This process, which was complete at ~250°C, corresponded to the loss of m ~ 5–8 molecules of adsorbed and crystal water, and it did not affect the heteropoly anion structure [19]. Only a small weight loss was observed on the subsequent heating of the samples. For $Cs_{2.5}H_{0.5}PMo_{12}O_{40}$ with supported H_2PtCl_6 (Table 1, no. 1), the continuous weight loss over the range of 220–500°C can correspond to the removal of HCl molecules and water formed upon the decomposition of the acid salt. For $Cs_{2.5}H_{0.5}PMo_{12}O_{40}$ coprecipitated with $Pt(NH_3)_4Cl_2$ (Table 1, no. 2), a pronounced endotherm was observed at 230°C, which corresponds to the removal of 0.4 molecules of NH_3 on the heteropoly anion basis. The diffuse peak at T_2 ~ 400°C might correspond to the removal of 0.2 molecules of HCl and structural water on heteropoly anion decomposition.

The thermal stability of heteropoly anions was studied in the absence of promoter additives. As the weight of $Cs_{2.5}H_{0.5}PMo_{12}O_{40} \cdot 3.8H_2O$ was increased to 1000 mg, we managed to monitor the release of structural water (Table 1, no. 3). The DTG curve exhibited a weak maximum at T_2 = 415°C; the DTA curve exhibited overlapping exo- and endothermic peaks detectable at 415 and 440°C (Fig. 2a). Bondareva et al. [20]

observed the same effects in the decomposition of the HPA $H_3PMo_{12}O_{40} \cdot 13H_2O$ and assigned them to the formation of the anhydride $H_xPMo_{12}O_{38.5+x/2}$ ($x \approx 0.1$) followed by its conversion into MoO_3. The similarity of the results of thermal analysis suggests the presence of $H_3PMo_{12}O_{40}$ in the acid cesium salt. After the decomposition of the acid, MoO_3 and the salt $Cs_3PMo_{12}O_{40}$, which exhibit high thermal stability, remained in the sample.

The true composition of acid cesium salts of $H_3PW_{12}O_{40}$ has been studied previously [4, 21, 22]. These salts can contain heteropoly anions with various degrees of protonation or can be fully substituted Cs salts in combination with an acid coprecipitated or crystallized in pores. In the hydrates of these salts, the H_3 acid was observed crystallographically at a sufficiently high concentration of protons (H^+/heteropoly anion ≥ 1.5) as a solid solution in a Cs_3 salt [21] or as an individual phase [4]. At a lower proton concentration, the H_3 acid was not detected. In a ^{31}P NMR-spectroscopic study of anhydrous $Cs_xH_{3-x}PW_{12}O_{40}$ samples, the occurrence of both Cs_3 and H_3 species and CsH_2 and Cs_2H acid salts, in which protons are localized at the bridging oxygen atoms of W–O–W, was demonstrated [22]. Thus, the results of our thermogravimetric analysis are consistent with published data on the occurrence of $H_3PMo_{12}O_{40}$ as the constituents of acid Cs salts. The formation of $H_3PMo_{12}O_{40}$ could also occur in the course of heating as a result of a redistribution of H^+ and Cs^+ ions.

The decomposition of the acid salts $Cs_xH_{3+n-x}PMo_{12-n}V_nO_{40} \cdot mH_2O$ was described by typical [9] DTG and DTA curves (Table 1, nos. 4–7; Fig. 2b). Weak maximums at $T_2 \sim 300$°C in DTG curves and weakly pronounced *endo* and *exo* effects in DTA curves corresponded to the removal of structural water. In some samples, thermal transitions unaccompanied by weight losses were observed at $T_3 \sim 500$°C. To determine the number of moles q of structural water released per mole of the acid salt, the range ΔT between the temperature of the completion of the release of crystal water (280 or 230°C in samples in Fig. 2) and the temperature at which a constant sample weight was reached (usually, ~500°C) was chosen in a DTG curve. The resulting values of q (Table 1) for $Cs_xH_{3+n-x}PMo_{12-n}V_nO_{40} \cdot mH_2O$ were noticeably lower than the values to be observed upon the complete removal of acid salt protons. Dimitratos and Vedrine [9] measured the amount of water released from $Cs_{2.5}H_{1.5}PMo_{11}VO_{40}$, and this amount corresponded to the complete removal of protons. The difference between data can be explained by different analysis conditions. It is likely that, under conditions of our measurements, a portion of protons remained in the samples of $Cs_xH_{3+n-x}PMo_{12-n}V_nO_{40} \cdot mH_2O$, and these protons formed highly substituted acid Cs salts with

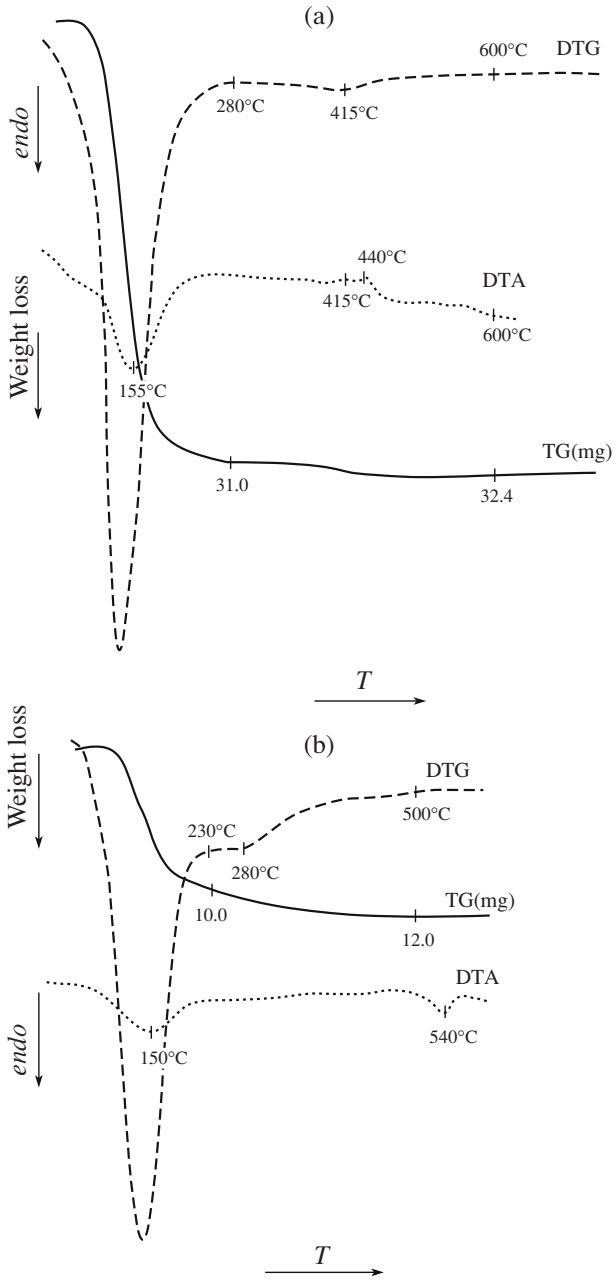

Fig. 2. Thermogravimetric curves of acid cesium salts of HPAs: (a) $Cs_{2.5}H_{0.5}PMo_{12}O_{40} \cdot 3.8H_2O$, sample weight of 1000 mg and (b) $Cs_{2.5}H_{3.5}PMo_9V_3O_{40} \cdot 6.0H_2O$, sample weight of 200 mg.

P–Mo–V heteropoly anions. It is well known that these compounds are sufficiently stable [19].

It is likely that the acid salts $Cs_xH_{3+n-x}PMo_{12-n}V_nO_{40}$ underwent deprotonation through the formation of corresponding acids because a weight loss maximum was observed at $T_2 \sim 300$°C, which is close to the temperature of the onset of decomposition of the acid $H_4PMo_{11}VO_{40}$, as determined by in

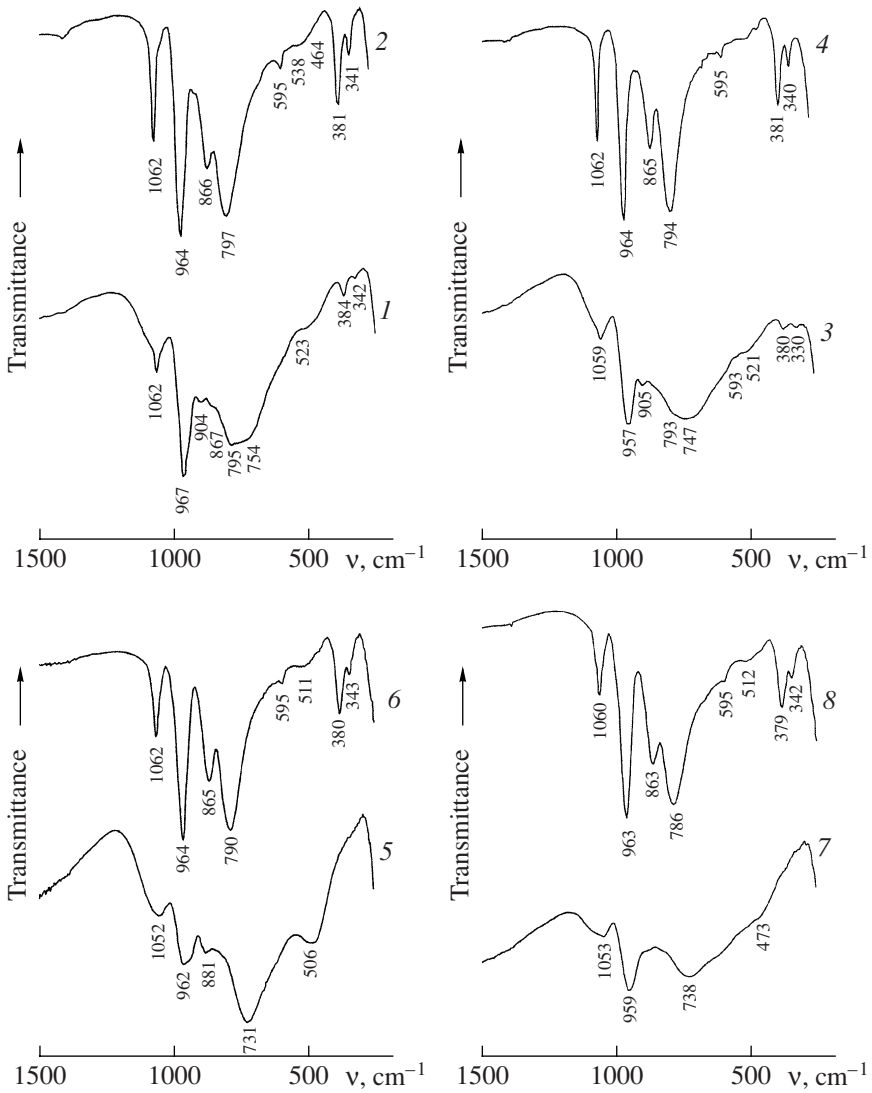

Fig. 3. IR spectra of the samples of platinum-promoted acid cesium salts of HPAs after reduction with hydrogen, catalytic reaction, and reoxidation: (*1*, *2*) $Pt_{0.1}$-$Cs_{2.5}H_{0.5}PMo_{12}O_{40}$ reduced in H_2 at 300°C and (*1*) kept in air for a day and (*2*) reoxidized upon storage in air for two months; (*3*, *4*) $Pt_{0.1}/Cs_{2.5}H_{0.5}PMo_{12}O_{40}$ after reduction in H_2 at 300°C, (*3*) kept in air for a day, and catalytic reaction and (*4*) reoxidized with oxygen at 300°C; (*5*, *6*) $Pt_{0.1}$-$Cs_{2.5}H_{2.5}PMo_{10}V_2O_{40}$ reduced in H_2 at 300°C and (*5*) kept in air for a day and (*6*) reoxidized with oxygen at 300°C; (*7*, *8*) $Pt_{0.1}/Cs_{2.5}H_{2.5}PMo_{10}V_2O_{40}$ after reduction in H_2 at 300°C, (*7*) kept in air for a day, and catalytic reaction and (*8*) reoxidized with oxygen at 300°C.

situ IR spectroscopy [23]. The decomposition mechanism of the acid $H_4PMo_{11}VO_{40}$ involved the release of vanadium from the heteropoly anion and a redistribution of molybdenum with the formation of the acid $H_3PMo_{12}O_{40}$, which is more thermally stable [23, 6]. According to our data, upon heating the acid salts $Cs_{2.5}H_{1.5}PMo_{11}VO_{40} \cdot 4.7H_2O$ and $Cs_{2.5}H_{2.5}PMo_{10}V_2O_{40} \cdot 5.4H_2O$ to 600°C, only a partial release of vanadium ions from the heteropoly anions occurred, as judged from the appearance of a very weak absorption band at 1035 cm^{-1} due to vanadyl phosphate with the retention of the IR spectra of the initial heteropoly anions as constituents of the thermally stable Cs salts [23]. Under the same conditions, as judged from the IR spectrum, the heteropoly anion of the salt $Cs_{2.5}H_{3.5}PMo_9V_3O_{40} \cdot 5.5H_2O$ was converted into the anion $PMo_{12}O_{40}^{3-}$ with the release of vanadium from the heteropoly anion.

Based on the above data, we can conclude that the region of the full thermal stability of acid Cs salts is limited by the decomposition temperatures of the corresponding HPAs: ~400°C for $H_3PMo_{12}O_{40}$ and ~300–350°C for $H_{3+n}PMo_{12-n}V_nO_{40}$.

Redox Transformations of Platinum-Promoted Acid Cesium Salts

Redox transformations were studied in two catalyst samples with coprecipitated platinum:

$Pt_{0.1}$-$Cs_{2.5}H_{0.5}PMo_{12}O_{40}$ (**1**) and $Pt_{0.1}$-$Cs_{2.5}H_{2.5}PMo_{10}V_2O_{40}$ (**2**). After treatment with hydrogen at 300°C for 1 h and exposure to air, the samples exhibited IR spectra (Fig. 3, spectra *1* and *5*) corresponding to the Keggin structure distorted by reduction [24]. Upon a long storage in air, the reduced heteropoly compounds were oxidized with the regeneration of their structures (Fig. 3, spectrum *2*). The oxidation process with the Keggin stricture regeneration was considerably accelerated as the temperature was increased to 300°C (Fig. 3, spectrum *6*). To solve the crucial problem of the retention of vanadium as a constituent of the heteropoly anion after the reduction–oxidation cycle, we analyzed the shapes of the ν(P–O) line in samples **1** and **2**. The heteropoly anion $PMo_{12}O_{40}^{3-}$ exhibits a narrow symmetric absorption band at 1062 cm^{-1}, which belongs to triply degenerate ν(P–O) vibrations (T_d symmetry). The degeneracy disappeared upon the replacement of metal ions in the composition of heteropoly anions [25]. Three ν(P–O) bands were observed in V-substituted heteropoly anions (Fig. 4). The parameters of these bands were similar for sample **2** in the initial state and after reduction (H_2, 300°C) followed by reoxidation in air (Figs. 4a, 4b). For sample **2**, the above three bands were observed after reduction and reoxidation at a high temperature (O_2, 300°C); in addition, two weak components due to heteropoly anion decomposition products at 1086 and 1033 cm^{-1} can be recognized (Fig. 4c). A noticeable difference in the intensities and positions ofν(P–O) for the initial and reoxidized (at 300°C) samples can be explained by the presence of small amounts of vanadium(IV) ions as heteropoly anion constituents in the latter case.

The samples prereduced with H_2 at 300°C and stored in air were studied using TPR. Before measurements, the samples were treated with oxygen at 300°C.

Platinum catalyzes the reduction of heteropoly anions with hydrogen [14]. At temperatures up to ~700°C, the reduction curves of **1** and **2** were approximated with three peaks (Figs. 5a, 5b). Table 2 summarizes the amounts of hydrogen calculated from these peak areas.

At the first step of reduction (T_{max} ~ 70°C), the sample of $Pt_{0.1}$-$Cs_{2.5}H_{0.5}PMo_{12}O_{40}$ (Figs. 5a, 5c) absorbed ~0.1 mol of H_2 per mole of the heteropoly compound. After the second step (T_{max} = 265°C), the total amount of absorbed H_2 was 2.2 mol per mole of the heteropoly compound. This corresponds to the reduction of ~4 ions of Mo(VI) to Mo(V) in the heteropoly anion. After the third step (T_{max} = 475°C), the absorption of H_2 corresponded to the complete reduction of Mo(VI) to Mo(IV), which should cause heteropoly anion decomposition. As the temperature was further increased, an even deeper reduction of molybdenum was observed.

The oxidizing power of $Pt_{0.1}$-$Cs_{2.5}H_{2.5}PMo_{10}V_2O_{40}$ (Figs. 5b, 5d) was higher because of the presence of vanadium(V) ions; therefore, the peak with T_{max} =

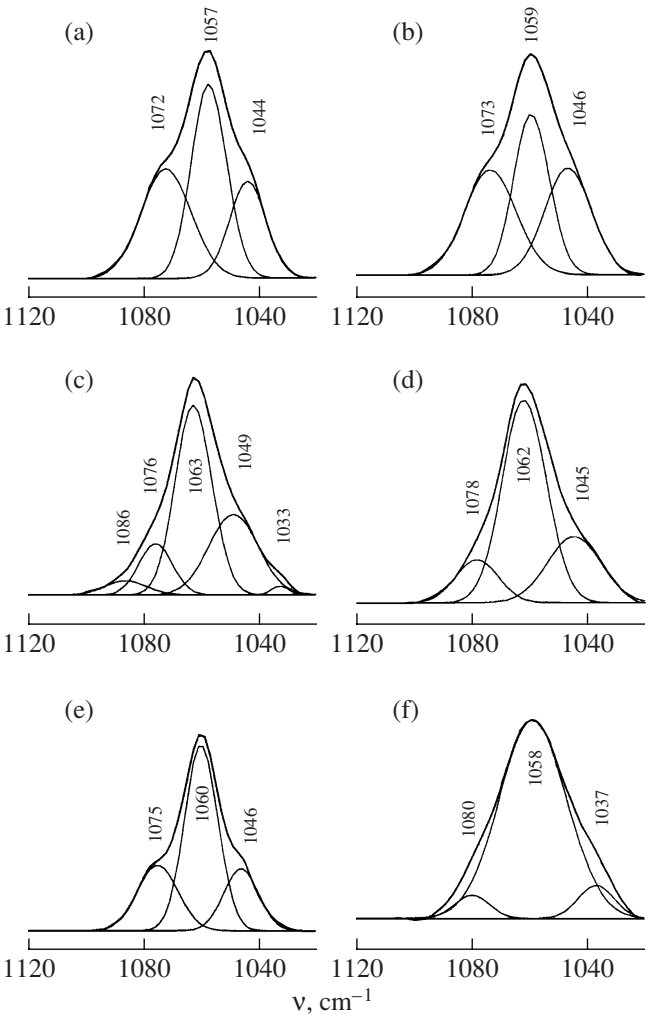

Fig. 4. Deconvolution of the ν(P–O) IR absorption band due to V-substituted heteropoly anions into individual components: (a) initial sample of $Pt_{0.1}$-$Cs_{2.5}H_{2.5}PMo_{10}V_2O_{40}$, (b) after reduction with hydrogen (300°C) and oxidation in air, (c) after reduction with hydrogen (300°C) and oxidation with oxygen at 300°C, (d) after reduction with hydrogen (200°C) and catalytic reaction, (e) initial sample of $Pt_{0.1}$-$Cs_{2.5}H_{1.5}PMo_{11}VO_{40}$, (f) after reduction with hydrogen (200°C) and catalytic reaction.

143°C corresponds to the absorption of ~4 mol of H_2 per mole of the heteropoly compound, and the vanadium-containing heteropoly anion occurred in a more reduced state in the low-temperature region. The next small peak with T_{max} = 238°C was observed against the background of an intense broad band with T_{max} = 480°C; it corresponded to the additional absorption of 0.5 mol of H_2 per mole of the heteropoly compound. After the third step, sample **2**, as well as sample **1**, was deeply reduced.

The reversibility of the redox transformations of platinum-promoted acid Cs salts of HPAs was tested after reduction to 360°C in order to avoid complete decomposition of the heteropoly anion (Figs. 5c, 5d,

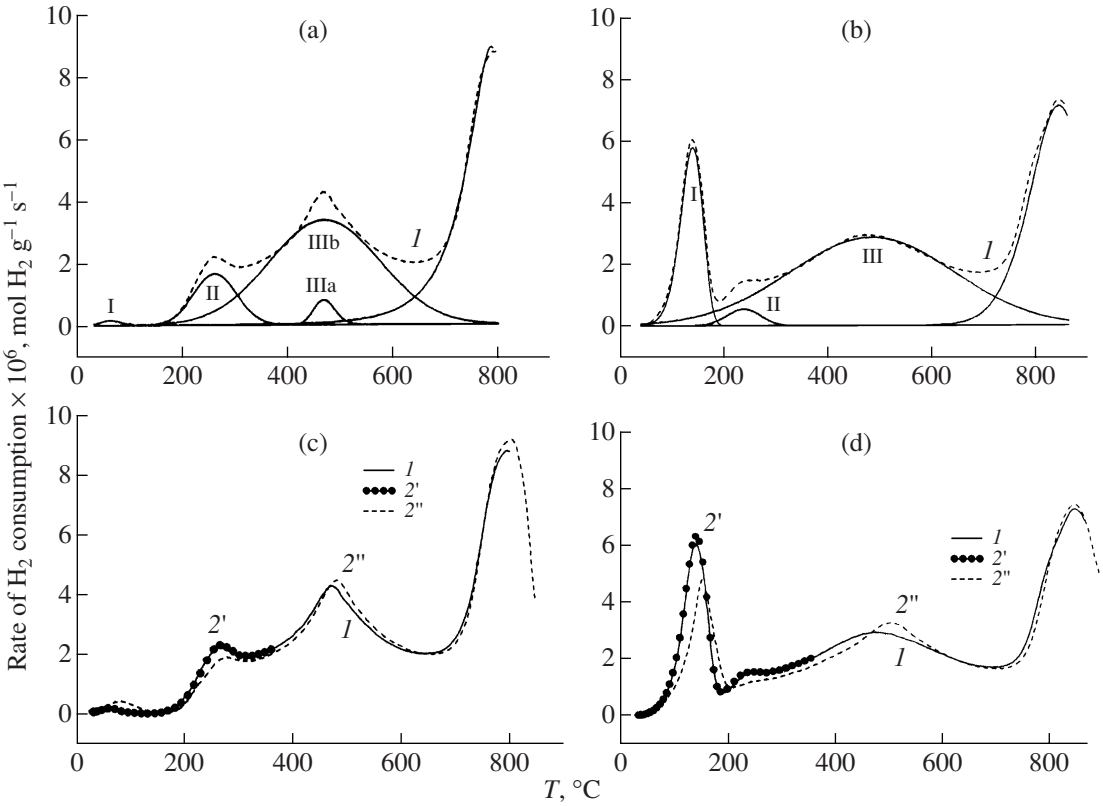

Fig. 5. TPR curves for the samples of (a, c) $Pt_{0.1}$-$Cs_{2.5}H_{0.5}PMo_{12}O_{40}$ and (b, d) $Pt_{0.1}$-$Cs_{2.5}H_{2.5}PMo_{10}V_2O_{40}$: (a, b) TPR curves of (*1*) initial heteropoly compounds and their approximation (peaks I–III); (c, d) test for the reversibility of redox transformations; (*1*) TPR up to ~800°C; (*2*') TPR of reoxidized sample *1* up to 360°C; (*2*'') TPR after the reoxidation of sample *2*'.

curves *2*'). After the first TPR (up to 360°C), the samples were reoxidized at 300°C and the repeated TPR was performed. As compared with the first cycle (Figs. 5c, 5d, curves *1*, *2*'), a satisfactory reproducibility of TPR was observed for $Pt_{0.1}$-$Cs_{2.5}H_{0.5}PMo_{12}O_{40}$ (Fig. 5c, curve *2*''). For $Pt_{0.1}$-$Cs_{2.5}H_{2.5}PMo_{10}V_2O_{40}$, more differences were observed in the repeated cycle (Fig. 5d, curve *2*''); this could be due to both the incomplete reoxidation of the sample and the partial decomposition of the heteropoly compound, which was also observed using IR spectra.

With the use of XPS, we analyzed the surfaces of samples $Pt_{0.1}$-$Cs_{2.5}H_{0.5}PMo_{12}O_{40}$ (**1**) and $Pt_{0.1}$-$Cs_{2.5}H_{2.5}PMo_{10}V_2O_{40}$ (**2**) reduced with H_2 at 300°C for 1 h and kept in air after the reduction. According to IR-spectroscopic data, heteropoly anions in samples **1** and **2** remained in a reduced state for a day (Fig. 3,

Table 2. Positions of TPR peaks (T_{max}), the amount of absorbed hydrogen, and the total number of moles of absorbed H_2 per mole of the heteropoly compound (sample weight of 1 g)

Heteropoly compound	Peak no.	T_{max}, °C	Amount of absorbed H_2	
			×10^6, mol H_2	$\frac{\sum(\text{mol } H_2)}{(\text{mol heteropoly compound})}$
$Pt_{0.1}$-$Cs_{2.5}H_{0.5}PMo_{12}O_{40}$	I	67	50.1	0.11
(**1**)	II	265	994	2.2
	III	475	5450	14
$Pt_{0.1}$-$Cs_{2.5}H_{2.5}PMo_{10}V_2O_{40}$	I	143	1860	3.9
(**2**)	II	238	264	4.5
	III	485	6750	18

Table 3. XPS data on binding energies and atomic ratios between the elements in the platinum-promoted samples of Cs salts reduced with hydrogen (300°C)*

No.	Sample	Binding energy, eV				Cs/Mo/V/O
		Mo 3*d*	O 1*s*	Cs $3d_{5/2}$	V 2*p*	
1	$Pt_{0.1}$-$Cs_{2.5}H_{0.5}PMo_{12}O_{40}$, r	232.3	530.6	724.1	–	3.7 : 12 : 0 : 38
2	$Pt_{0.1}$-$Cs_{2.5}H_{0.5}PMo_{12}O_{40}$, o	233.0	530.8	724.1	–	2.9 : 12 : 0 : 49
3	$Pt_{0.1}$-$Cs_{2.5}H_{2.5}PMo_{10}V_2O_{40}$, r	232.3	530.3	724.0	515.9	5.5 : 10 : 2.2 : 36
4	$Pt_{0.1}$-$Cs_{2.5}H_{2.5}PMo_{10}V_2O_{40}$, r-o	232.8	530.6	724.1	516.5	3.3 : 10 : 2.9 : 49
5	$Pt_{0.1}$-$Cs_{2.5}H_{2.5}PMo_{10}V_2O_{40}$, o	233.1	530.8	724.1	517.2	4.0 : 10 : 2.5 : 45
6	$Cs_{2.5}H_{2.5}PMo_{10}V_2O_{40} \cdot 5.4H_2O$, i**	233.1	530.8	724.0	517.5	2.6 : 10 : 2.7 : 47

* The samples were kept in air for (r) a day, (r-o) a month, or (o) two months.

** Initial sample.

spectra *1* and *5*); however, they were almost completely oxidized after storage for two months.

According to XPS data, the Mo 3*d* binding energy in reduced sample **1** (Table 3, no. 1) was lower than the well-known value of 233.6 eV, which corresponds to the Mo(VI) state in $H_3PMo_{12}O_{40}$ [14]. A lower Mo3*d* binding energy was also observed in reduced sample **2**, as compared with the initial sample (Table 3, nos. 3 and 6). Moreover, the V2*p* binding energy decreased from 517.5 eV (Table 3, nos. 3 and 6) to 515.9 eV upon the reduction of sample **2**; it is likely that the latter value belongs to the vanadium(IV) state. The exposure of prereduced samples to air caused their oxidation, as evidenced by an increase in the binding energies of molybdenum and vanadium (Table 3, nos. 2, 4, and 5). Figure 6 shows the observed Mo3*d* XPS spectra and the results of their deconvolution into individual doublets. In the samples reduced at 300°C (Figs. 6a, 6b), the major portion of molybdenum occurred in the Mo(V) state characterized by a Mo binding energy of ~232 eV [14]. A component of ~230 eV, which can belong to more deeply reduced molybdenum, was also present. After reoxidation in air, the samples contained Mo(VI) ions (~233 eV) as the constituents of regenerated heteropoly anions and only a small fraction of Mo(V) (Figs. 6c, 6d). Based on the V 2*p* binding energy, reoxidized sample **2** contained vanadium(V) and an impurity of vanadium(IV) (517.2 against 517.5 eV in the starting heteropoly anion).

Thus, the oxidation states of molybdenum and vanadium on the surface determined using XPS correspond to the formation of reduced or reoxidized heteropoly anions in the bulk of the samples, which were characterized using TPR and IR spectroscopy.

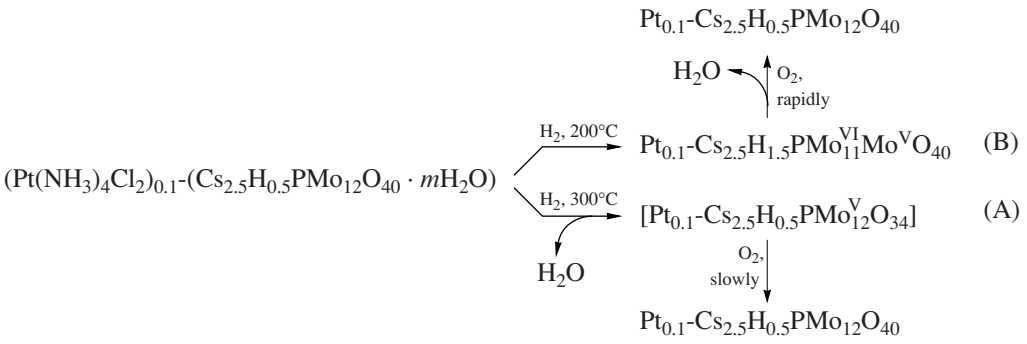

Scheme. Redox transformations of the acid Cs salt of molybdophosphoric HPA (**1**).

The scheme shows the reduction and reoxidation of sample **1**. The treatment of the platinum-containing cesium salt with hydrogen at 300°C resulted in the deep but reversible reduction of the heteropoly anion accompanied by the release of several oxygen ions as the constituents of water molecules and the formation of hypothetical species A. The oxidation of deeply reduced heteropoly anions with oxygen occurs slowly because it is associated with the regeneration of the Keggin structure [26]. The treatment of acid Cs salts with hydrogen was also performed at 200°C. In this case, in sample **1**, a small number of molybdenum ions (~1) were reduced to form heteropoly anion species B (scheme). According to TPR data, vanadium-containing sample **2** was

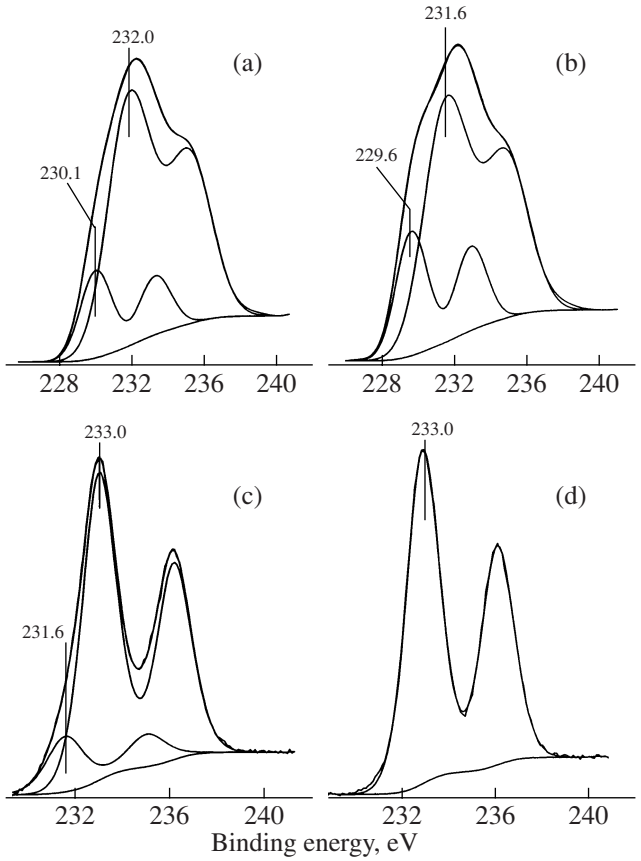

Fig. 6. Deconvolution into individual components of the Mo 3*d* region in the XPS spectra of the samples of (a, c) $Pt_{0.1}$-$Cs_{2.5}H_{0.5}PMo_{12}O_{40}$ and (b, d) $Pt_{0.1}$-$Cs_{2.5}H_{2.5}PMo_{10}V_2O_{40}$ after reduction with hydrogen at 300°C and storage in air for (a, b) a day or (c, d) two months.

more deeply reduced under the same conditions. It contained vanadium(IV) ions and a small quantity Mo(V) ions. The heteropoly anions reduced at 200°C did not undergo considerable structural changes, and they were rapidly oxidized with oxygen, as evidenced by the IR spectra of the initial and reoxidized samples.

Under the action of hydrogen, platinum was reduced to metal, as demonstrated below for sample **1** reoxidized in air. Platinum metal activates molecular hydrogen; because of this, the reduction of heteropoly anions occurs at lower temperatures [14]. It is likely that it also activates molecular oxygen in the course of heteropoly anion reoxidation.

Table 3 summarizes the ratios between the elements on the surfaces of samples **1** and **2**, as determined from the integrated intensities of XPS signals. The found Mo/O and Mo/V/O ratios are approximately consistent with the bulk concentrations of these elements. However, according to XPS data, the Cs/Mo ratio for reduced samples is higher by a factor of ~2 than that specified by the formulas of **1** and **2**. This can be explained by the concentration of Cs^+ ions in the near-surface layers of highly reduced samples. We failed to

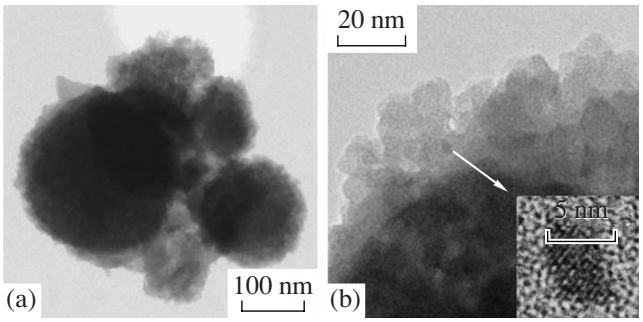

Fig. 7. HRTEM images of the sample of $Pt_{0.1}$-$Cs_{2.5}H_{0.5}PMo_{12}O_{40}$: (a) the globular morphology of the salt $Cs_{2.5}H_{0.5}PMo_{12}O_{40}$; (b) Pt metal as a constituent of the sample (the insert shows the micrograph of a Pt particle with the interplanar spacing d_{111} = 0.227 nm).

detect the Pt 4*f* XPS signals because they were masked by the Cs 4*d* signals. The Pt 3*d* signal of a lower intensity did not exceed the noise level.

High-Resolution Transmission Electron Microscopy

The states of components were studied by HRTEM using prereduced $Pt_{0.1}$-$Cs_{2.5}H_{0.5}PMo_{12}O_{40}$ (**1**) reoxidized in air. In the micrograph, two clearly different texture levels can be distinguished: coarse particles of the salt $Cs_{2.5}H_{0.5}PMo_{12}O_{40}$ with a globular morphology 100–300 nm in diameter (Fig. 7a) and spherical nanoparticles 10–20 nm in size. The latter can be clearly seen at the rough edges of coarse particles; this allowed us to assume that the coarse particles are aggregates of small particles. The individual Keggin ions with a characteristic size of ~1 nm cannot be seen in the micrographs, and the observed particles of size 10–20 nm are the associates of individual heteropoly compound particles.

At the edges of heteropoly compound associates, Pt nanoparticles in a metal state of size 5 nm or smaller can be detected. In the micrographs, these particles are observed as more contrasting small spots (Fig. 7b); at a larger magnification, they give an image of platinum lattice planes with the interplanar spacing d_{111} = 0.227 nm. The size of the detected particles indicates a fairly high degree of dispersion of platinum.

Texture Characteristics of Platinum-Promoted Acid Cesium Salts

The specific surface areas and pore size distributions of acid cesium salts of the HPA $H_3PW_{12}O_{40}$ have been studied previously [3–5, 27], and Lee et al. [6] measured the specific surface areas of the salts $Cs_xH_{3-x}PMo_{11}VO_{40}$. We studied in more detail the pore structure of the platinum-promoted acid cesium salts $Cs_xH_{3+n-x}PMo_{12-n}V_nO_{40}$ (x = 2.5 or 3.5; n = 0, 1, 2, or 3). The adsorption studies were performed with a few series of samples prepared by platinum coprecipi-

Table 4. Specific surface areas of platinum-promoted acid cesium salts and the yields of phenol in the benzene oxidation reaction at the points in time specified in parentheses at the beginning and the end of measurements

No.	Catalyst*	S_{BET}, m^2/g	S_α, m^2/g	Yield of phenol $\times 10^4$, mol/h	
				initial (min)	final (min)
1	$Pt_{0.1}$-$Cs_{2.5}H_{0.5}PMo_{12}O_{40}$ (I)	148	140	1.10 (75)	0.89 (190)
2	The same	–	–	0.99 (110)	0.79 (290)
3	The same	–	–	0.86 (65)	0.74 (100)
4	$Pt_{0.1}$-$Cs_{2.5}H_{0.5}PMo_{12}O_{40}$ (II)	162	118	1.30 (30)	1.20 (210)
5	$Pt_{0.02}$-$Cs_{2.5}H_{0.5}PMo_{12}O_{40}$	172	159	1.80 (80)	1.80 (240)
6	$Pt_{0.1}/Cs_{2.5}H_{0.5}PMo_{12}O_{40}$	14.7	10.9	2.00 (55)	1.70 (225)
7	$Pt_{0.1}$-$Cs_{2.5}H_{1.5}PMo_{11}VO_{40}$	154	72	0.44 (55)	0.28 (120)
8	$Pt_{0.1}$-$Cs_{2.5}H_{2.5}PMo_{10}V_2O_{40}$	84	48	0.58 (30)	0.53 (135)
9	$Pt_{0.1}$-$Cs_{2.5}H_{3.5}PMo_9V_3O_{40}$	75	13	0.07 (30)	0.09 (70)
10	$Pt_{0.1}/Cs_{2.5}H_{2.5}PMo_{10}V_2O_{40}$	26	8.5	0.09 (60)	0.09 (160)
11	$Pt_{0.1}/Cs_{3.5}H_{0.5}PMo_{11}VO_{40}$	53	38	0.20 (40)	0.20 (100)
12	$Pt_{0.1}/Cs_{3.5}H_{1.5}PMo_{10}V_2O_{40}$	112	58	0.46 (50)	0.41 (85)
13	$Pt_{0.1}/Cs_{3.5}H_{2.5}PMo_9V_3O_{40}$	109	10	0.31 (60)	0.19 (165)

Note: Catalytic measurement conditions: 0.3 g of a catalyst reduced with H_2 at 300°C was used; the reaction temperature was 180°C; the gas flow rates in the reaction mixture of $H_2/O_2/C_6H_6/N_2$ were 10, 5, 8, and 85 ml/min, respectively.
* Sample nos. 1 and 3 were tested after a month and ~1 h, respectively; the other samples were tested a day after reduction with hydrogen.

tation or supporting, including the study of samples after reduction and catalytic tests. Adsorbed and crystal water was removed upon the treatment of the samples at 150°C.

For the initial samples, Table 4 summarizes the independently measured specific surface areas S_{BET} and S_α. They were independent because different segments of nitrogen adsorption isotherms were used to calculate them [16, 17]. It is well known that $S_{BET} \approx S_\alpha$ or $S_{BET} > S_\alpha$ in the absence or in the presence of micropores, respectively. In these cases, the value of S_α corresponds to the specific surface area of mesopores that remained after the filling of micropores.

The samples prepared by platinum coprecipitation from a solution of a HPA and $Pt(NH_3)_4Cl_2$ exhibited high specific surface areas S_{BET} (Table 4, nos. 1, 4, 5, 7–9). Good data reproducibility is observed: for three Pt-$Cs_{2.5}H_{0.5}PMo_{12}O_{40}$ samples Table 4, nos. 1, 4, 5) S_{BET} = 150–170 m^2/g. The specific surface area of samples coprecipitated with platinum (Table 4, nos. 7–9) decreased with the introduction of one to three vanadium(V) ions into the heteropoly ion (which was accompanied by an increase in the number of acid protons). The samples prepared by the impregnation of solid $Cs_{2.5}H_{0.5}PMo_{12}O_{40}$ (S_{BET} = 150 m^2/g) and $Cs_{2.5}H_{2.5}PMo_{10}V_2O_{40}$ (S_{BET} = 92 m^2/g) with a solution of the H_2PtCl_6 acid exhibited low specific surface areas (Table 4, nos. 6, 10) unlike the samples with coprecipitated platinum (Table 4, nos. 4, 8). At the concentration of Cs^+ corresponding to $x = 3.5$, an increase in the number of vanadium ions and protons (Table 4, nos. 11–13) resulted in an increase in the values of S_{BET}. At the same time, on going to V-substituted heteropoly anions, the fraction of micropores increased, and the fraction of S_α with respect to the total specific surface area correspondingly decreased (Table 4, nos. 1, 4, 5, 7–9, and 10–13).

With the accessibility of the surfaces of all individual heteropoly anions with a characteristic diameter of ~1 nm, the specific geometric surface areas (S_0) are related to particle diameter (D_0) and true density (ρ) by a relationship that has the following form for spherical particles [16, 17]:

$$S_0 = \frac{6}{D_0\rho}. \quad (1)$$

Our measurements of the true helium density ρ of the salt $Cs_{2.5}H_{0.5}PMo_{12}O_{40} \cdot 3.8H_2O$ gave a value of 4.305 g/cm^3. From the formula composition of this salt, it follows that its dehydration, as well as the introduction of small amounts of Pt, will not cause considerable changes in ρ. The use of the above value of ρ and D_0 = 1 nm gave S_0 = 1394 m^2/g, which is larger than the experimental specific surface areas by one order of magnitude. These estimations allowed us to assume that heteropoly compounds are closely associated to primary texture particles. The space inside these particles is almost inaccessible to nitrogen molecules at 77 K, and its small accessible portion manifests itself as the micropore volume V_μ. In this case, the surface area

Table 5. Comparison between the texture characteristics of samples before and after catalytic tests or additional treatments

Sample*	S_{BET}, m^2/g	S_α, m^2/g	V_Σ, cm^3/g	V_μ, cm^3/g	V_{10}, cm^3/g	d_1, nm	V_{100}, cm^3/g	d_2, nm
4	162	140	0.151	0.022	0.091	<4	0.060	**
4-*t*	149	143	0.158	0.063	0.086	3.5	0.072	**
4-*u*	4.0	4.0	0.034	0.000	0.0006	7.0	0.033	40–50
5	172	159	0.223	0.008	0.102	3.5	0.121	40
5-*h*	103	126	0.142	0.000	0.067	3.5	0.075	40
5-*u*	11.5	12.1	0.078	0.000	0.004	3.5	0.074	40
6	14.7	10.9	0.060	0.003	0.004	3.5	0.056	25
6-*u*	3.8	2.5	0.054	0.0006	0.000	no	0.054	20
10	26.4	25.1	0.032	0.001	0.020	4.0	0.012	**
10-*u*	~1	~2	0.010	0.000	0.002	7–8	0.008	20–30

* Sample numbers are the same as in Table 4. Numbers without a letter refer to initial samples; the letters *u*, *t*, and *h* indicate samples after reaction, after conditioning at 300°C before adsorption measurements, and after reduction with H_2 at 300°C and keeping in air, respectively.

** Without a pronounced maximum.

S_α corresponds to the outer surface of primary texture particles, whereas the surface area S_{BET} corresponds to the total accessible surface including the micropore surface. The average size D_1 of primary texture particles, which are spherical according to HRTEM data, can be estimated from Eq. (1) on substituting the values of S_α in it and replacing ρ with $\rho(1-\varepsilon_\mu)$, where ε_μ is the inner porosity of primary texture particles [17]. The estimated size of these particles at $\varepsilon_\mu < 0.5$, which corresponds to close packings, and S_α of ~120–160 m^2/g (Table 4, nos. 1, 4, and 5) gives D_1 of ~10–20 nm, which is consistent with the size of heteropoly compound nanoparticles observed by HRTEM.

The occurrence of two texture levels for heteropoly compounds of this type ($(NH_4)_3PW_{12}O_{40}$) is well known [28], and it was supported by our results of adsorption studies concerning pore size distributions. In typical cases, two distribution maximums were observed: in the regions of pores with characteristic sizes $d_1 \sim 3.5$ nm and $d_2 \sim 20$–50 nm. It is reasonable to identify smaller pores with spaces between closely packed primary texture particles of size ~10–20 nm and larger pores with spaces between particles of size ~100–300 nm. Note that these ratios between pore and particle sizes in combination with the close packing of heteropoly compounds in primary texture particles suggest a high packing density of these compounds at all levels.

Table 5 summarizes the most complete pore structure characteristics for the chosen samples. The sample numbers correspond to those specified in Table 4. In addition to the values of S_{BET} and S_α, the total pore volume V_Σ with effective sizes up to 100–200 nm and the micropore volume V_μ are given. The volume V_{10} of pores with characteristic sizes to 10 nm, the volume V_{100} of pores with sizes greater than 10 nm, and the corresponding pore diameters d_1 and d_2 at distribution maximums are also given.

The thermal treatment of the catalyst caused slight changes in the texture characteristics (samples 4 and 4-*t*), whereas the reduction with hydrogen more significantly decreased the specific surface area and pore volume at both levels and removed microporosity (samples 5 and 5-*h*). In this case, an agglomeration of spherical particles of size ~10 nm can be observed in the HRTEM image (Fig. 7); however, in general, the globular character of the texture of heteropoly compounds was retained after reduction. Changes that are more radical occurred in the catalytic tests of the deeply reduced heteropoly compounds $Cs_{2.5}H_{0.5}PMo_{12}O_{40}$ with both coprecipitated and supported platinum and V-containing heteropoly compounds (samples 4-*u*, 5-*u*, 6-*u*, and 10-*u*). The changes consisted in a decrease in the specific surface area, which is characteristic of the agglomeration process (the values of S_{BET} and S_α decreased by almost one order of magnitude), and the volume of fine pores of size to 10 nm at small changes in the pore volume V_{100} between coarse particles of heteropoly compounds. As found by the analysis of sample 4-*u* performed after a long storage in air, the resulting pore structure changes were irreversible, although the Keggin structure of the heteropoly anion was completely regenerated upon storage.

We failed to find published data on deep texture changes of this kind under catalytic reaction conditions. The mechanisms of these changes should be further studied in detail. As a first approximation, we can assume that heteropoly compounds are associated in spherical primary particles by electrostatic and hydrogen bonds. A change in the composition and charge type of heteropoly compounds can increase the size of associates, analogously to agglomeration. In this case,

the retention or subsequent regeneration of the molecular structure of the heteropoly compound is possible. These transformations are facilitated by the high packing density of heteropoly compounds at all texture levels; it is likely that the formation of water molecules in the course of a catalytic reaction facilitates these transformations.

Benzene Oxidation with an $O_2 + H_2$ Mixture in the Presence of the Acid Cesium Salts $Cs_xH_{3+n-x}PMo_{12-n}V_nO_{40}$ ($n = 0, 1, 2,$ or 3; $x = 2.5$ or 3.5) and Platinum

As found previously, the samples containing platinum and heteropoly compounds acquired catalytic activity in the gas-phase reaction of benzene oxidation with an $O_2 + H_2$ mixture only after prereduction with hydrogen with the formation of platinum metal [12–14]. After the hydrogen treatment of the Pt–Cs salts of P–Mo–V HPAs at 300°C and storage in air, platinum metal was present in the samples in accordance with HRTEM data. According to the results obtained by TPR, IR spectroscopy, and XPS, heteropoly anions were deeply reduced with hydrogen both on the surface and in the bulk of the samples, and they were slowly reoxidized with oxygen with the retention of the composition. The activity of these catalysts in the oxidation of benzene with an $O_2 + H_2$ mixture was evaluated from the amount of the reaction product, phenol (mol/h). Table 4 summarizes the amounts of phenol for the initial period of measurements (~30–110 min after the admission of the reaction mixture) and at the end of tests (after 70–300 min). In the specified time interval, the yield of phenol moderately decreased or remained constant.

The salt $Cs_{2.5}H_{0.5}PMo_{12}O_{40}$ with coprecipitated platinum after reduction with hydrogen at 300°C and exposure to air for ~1 h, a day, and a month exhibited approximately the same catalytic activity (Table 4, nos. 1–3). Other samples were tested after reduction at 300°C and storage in air for a day. Using $Pt_{0.1}$-$Cs_{2.5}H_{0.5}PMo_{12}O_{40}$ as an example (Table 4, nos. 2 and 4), the adequate reproducibility of activity upon repeated syntheses of samples **I** and **II** was demonstrated.

In all of the samples (Table 4), CO_2 was the main oxidation by-product and the selectivity of benzene conversion into CO_2 was 50–60%.

The specific surface areas of samples decreased in the reaction atmosphere (Table 5, nos. 4–6, 10). It is likely that the pore structure of the catalyst was rearranged under the action of water formed in the reaction at 180°C.

To compare catalysts with different compositions, we calculated the specific catalytic activity as the ratio of the yield of phenol to the specific surface area of mesopores S_α measured after the experiment. For $Pt_{0.1}$-$Cs_{2.5}H_{0.5}PMo_{12}O_{40}$ (Table 4, no. 4), the specific catalytic activity was 1.1×10^{-4} mol h^{-1} m^{-2}. As the concentration of coprecipitated platinum was decreased by a factor of 5 in the sample of $Pt_{0.02}$-$Cs_{2.5}H_{0.5}PMo_{12}O_{40}$ (Table 4, no. 5), the specific catalytic activity decreased by a factor of only 2 to 0.5×10^{-4} mol h^{-1} m^{-2}. The disproportionate change in the specific catalytic activity can be explained by an increase in the degree of dispersion of platinum with decreasing platinum content of the samples, as was also observed for the catalyst Pt-$H_3PMo_{12}O_{40}/SiO_2$ [13]. For the sample $Pt_{0.1}/Cs_{2.5}H_{0.5}PMo_{12}O_{40}$, with platinum supported onto a heteropoly compound (Table 4, no. 6), the specific catalytic activity was 2.7×10^{-4} mol h^{-1} m^{-2}. This value is higher than that for the sample with the same concentration of coprecipitated platinum by a factor of ~2.5; this fact can be explained by the probable occurrence of platinum metal particles on the surface accessible to reactants rather than in the bulk of the catalyst. The activity of catalysts decreased with the introduction of vanadium ions. In the sample $Pt_{0.1}/Cs_{2.5}H_{2.5}PMo_{10}V_2O_{40}$, with platinum supported onto a heteropoly compound (Table 4, no. 10), the specific catalytic activity was $\approx 0.3 \times 10^{-4}$ mol h^{-1} m^{-2}.

It is of interest to compare the activity of the platinum-promoted Cs salts of HPAs in benzene oxidation to phenol with that of the supported Pt–HPA catalysts studied previously [13]. For the most active samples of 0.2% Pt–20% $H_3PMo_{12}O_{40}/SiO_2$ with developed surface areas of 400 and 200 m^2/g, the yield of phenol was 300 mol (g Pt)$^{-1}$ h^{-1}. For $Pt_{0.02}$-$Cs_{2.5}H_{0.5}PMo_{12}O_{40}$ with a specific surface area of 12 m^2/g, the yield of phenol was 60 mol (g Pt)$^{-1}$ h^{-1}. It is likely that the Cs salts were more active in terms of unit surface area of the catalyst because of the better contact between platinum particles and heteropoly compounds.

The IR spectra of catalyst samples measured after the reaction (Fig. 3, spectra *3* and *7*) indicate that the state of heteropoly anions remained unchanged; they remained deeply reduced, as were the initial species prereduced with hydrogen at 300°C (Fig. 3, spectra *1* and *5*). This can be explained by the fact that the oxidation of deeply reduced heteropoly anions (species A) with oxygen did not occur in the course of catalytic reaction in the presence of an $O_2 + H_2$ mixture.

Because partially reduced heteropoly anions are readily reoxidized with oxygen with the retention of the Keggin structure, we studied the IR spectra and catalytic properties of a series of platinum-promoted Cs salts of P–Mo–V HPAs weakly reduced at a low temperature (200°C) (species B). In this case, the IR spectra of the samples $Pt_{0.1}$-$Cs_{2.5}H_{0.5}PMo_{12}O_{40}$ and $Pt_{0.1}$-$Cs_{2.5}H_{0.5+n}PMo_{12-n}V_nO_{40}$ (n = 1 or 2) measured a day after reduction and after subsequent catalytic tests were identical and characteristic of Keggin structure heteropoly anions (Fig. 1, spectra *5–7*). Vanadium remained a constituent of the heteropoly anion, as judged from the presence of three absorption bands in the ν(P–O) region of heteropoly anions in the spectra

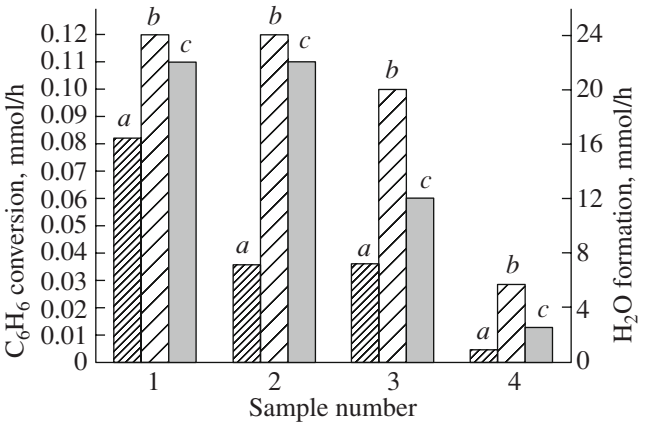

Fig. 8. Benzene conversion into (*a*) phenol and (*b*) CO_2 and water formation in the oxidation of benzene with an O_2 + H_2 mixture in the presence of the platinum-promoted Cs salts of HPAs: (*1*) $Pt_{0.1}$-$Cs_{2.5}H_{0.5}PMo_{12}O_{40}$, (*2*) $Pt_{0.1}$-$Cs_{2.5}H_{1.5}PMo_{11}VO_{40}$, (*3*) $Pt_{0.1}$-$Cs_{2.5}H_{2.5}PMo_{10}V_2O_{40}$, and (*4*) $Pt_{0.1}$-$Cs_{2.5}H_{3.5}PMo_9V_3O_{40}$. Reaction conditions: 0.1 g of a catalyst reduced with H_2 at 200°C was used; the reaction temperature was 180°C; the reaction flow rates (ml/min) of $H_2/O_2/C_6H_6/N_2$ were (*1*) 20, 10, 8, and 178; (*2*) 18, 9, 8, and 181; (*3*) 16, 8, 8, and 184; or (*4*) 12, 6, 8, and 190.

(Fig. 4, spectra *4* and *6*). The difference from the initial samples (Fig. 1, spectra *1–3*) consists in the lower relative intensity of the absorption band at ~860 cm^{-1} due to bridging oxygen atoms; this is associated with the presence of only a small amount of Mo(V) or V(IV) ions in the heteropoly anions. Under the same conditions, the sample of $Pt_{0.1}$-$Cs_{2.5}H_{3.5}PMo_9V_3O_{40}$ was more deeply reduced (Fig. 1, spectra *8* and *4*).

To compare the activities of a series of samples weakly reduced at 200°C, the yields of phenol, CO_2, and water were determined at the same oxygen and hydrogen concentrations at the reactor outlet; this was performed by varying the gas flow rates of O_2 and H_2 (Fig. 8). The yield of phenol determined at the steady-state regions of the reaction changed with changes in the composition of heteropoly anions (Fig. 8, *a*). The salt $Pt_{0.1}$-$Cs_{2.5}H_{0.5}PMo_{12}O_{40}$ gave a higher yield of phenol than $Pt_{0.1}$-$Cs_{2.5}H_{1.5}PMo_{11}VO_{40}$ at the same amounts of CO_2 and H_2O formed (samples *1* and *2*). The yield of phenol in the presence of $Pt_{0.1}$-$Cs_{2.5}H_{2.5}PMo_{10}V_2O_{40}$ (sample *3*) was somewhat higher than that in the presence of $Pt_{0.1}$-$Cs_{2.5}H_{1.5}PMo_{11}VO_{40}$ (sample *2*) with lower yields of CO_2 and H_2O. The salt $Pt_{0.1}$-$Cs_{2.5}H_{3.5}PMo_9V_3O_{40}$ (sample *4*) was almost inactive. For weakly reduced heteropoly compounds, the fraction of CO_2 in the products was higher than that for deeply reduced samples of the same heteropoly compounds. The selectivity of benzene conversion into CO_2 amounted to 60–80% based on the total benzene conversion into phenol and CO_2. Under these conditions, the conversion of benzene was 2.5%, as calculated from the yield of products, for $Pt_{0.1}$-$Cs_{2.5}H_{0.5}PMo_{12}O_{40}$; this value is close to the conversion on deeply reduced samples.

Another order of activity for the salts $Pd_{0.08}Cs_{2.5}H_{0.34+n}PMo_{12-n}V_nO_{40}$ (n = 0–3) was obtained in the oxidation of methane to formic acid with an $O_2 + H_2$ mixture at 300°C [10]. The conversion of methane increased with the number of vanadium ions over the range of 0.08–0.14%. As found using IR spectroscopy, vanadium left the heteropoly anion under reaction conditions. As a result, activity was actually measured in the presence of a weakly reduced Cs salt of molybdophosphoric acid containing palladium with other vanadium compound additives. Based on published data [10], which were obtained under conditions close to the conditions of our experiments (at 200°C), we can conclude that the palladium-promoted salt $Cs_{2.5}H_{0.5}PMo_{12}O_{40}$ was somewhat more active in this oxidation reaction with an $O_2 + H_2$ mixture than the palladium-promoted salt of the V-containing heteropoly anion $Cs_{2.5}H_{1.5}PMo_{11}VO_{40}$.

CONCLUSIONS

The resulting physicochemical characteristics of the acid salts $Cs_xH_{3+n-x}PMo_{12-n}V_nO_{40}$ (n = 0, 1, 2, or 3) promoted with platinum by coprecipitation or supporting are of importance for evaluating the applicability of these materials as catalysts for gas-phase oxidation reactions.

Using the oxidation reaction of benzene with an $O_2 + H_2$ mixture as an example, we found that the catalytic properties of platinum-containing acid cesium salts of molybdophosphoric and molybdovanadophosphoric HPAs depend on (1) the composition and reversible structural changes upon the reduction of Keggin heteropoly anions; (2) the presence of finely dispersed platinum metal in contact with a heteropoly compound, which is responsible for the reductive activation of oxygen as an oxidizing agent on the catalyst; and (3) the texture of catalysts, which is formed by the primary associates of individual heteropoly compounds and their secondary aggregates. In general, levels 1 and 2, which depend on the chemical composition, are responsible for potential catalytic activity, whereas level 3, which depends on the aggregation of heteropoly compound particles, is responsible for the accessible specific surface area and the actual catalytic activity.

REFERENCES

1. Misono, M., *Chem. Commun.*, 2001, no. 13, p. 1141.
2. Okuhara, T., Mizuno, N., and Misono, M., *Appl. Catal., A*, 2001, vol. 222, nos. 1–2, p. 63.
3. Volkova, G.G., Plyasova, L.M., Shkuratova, L.N., Budneva, A.A., Paukshtis, E.A., Timofeeva, M.N., and Likholobov, V.A., *Stud. Surf. Sci. Catal.*, 2004, vol. 147, p. 403.

4. Volkova, G.G., Plyasova, L.M., Salanov, A.N., Kustova, G.N., Yurieva, T.M., and Likholobov, V.A., *Catal. Lett.*, 2002, vol. 80, nos. 3–4, p. 175.
5. Yoshinaga, Y., Suzuki, T., Yoshimune, M., and Okuhara, T., *Top. Catal.*, 2002, vol. 19, no. 2, p. 179.
6. Lee, K.Y., Oishi, S., Igarashi, H., and Misono, M., *Catal. Today*, 1997, vol. 33, p. 183.
7. Misono, M., *Top. Catal.*, 2002, vol. 21, nos. 1–3, p. 89.
8. Min, J.-S. and Mizuno, N., *Catal. Today*, 2001, vol. 71, nos. 1–2, p. 89.
9. Dimitratos, N. and Vedrine, J.C., *Catal. Today*, 2003, vol. 81, no. 4, p. 561.
10. Min, J.-S., Ishige, H., Misono, M., and Mizuno, N., *J. Catal.*, 2001, vol. 198, no. 1, p. 116.
11. Popova, G.Ya., Andrushkevich, T.V., Bondareva, V.M., and Zakharov, I.I., *Kinet. Katal.*, 1994, vol. 35, no. 1, p. 91.
12. Kuznetsova, N.I., Kuznetsova, L.I., and Likholobov, V.A., *Katal. Prom–sti.*, 2003, no. 4, p. 17.
13. Kuznetsova, N.I., Kuznetsova, L.I., Likholobov, V.A., and Pez, G.P., *Catal. Today*, 2005, vol. 99, nos. 1–2, p. 193.
14. Kuznetsova, L.I., Kuznetsova, N.I., Koshcheev, S.V., Rogov, V.A., Zaikovskii, V.I., Novgorodov, B.N., Detusheva, L.G., Likholobov, V.A., and Kochubei, D.I., *Kinet. Katal.*, 2006, vol. 47, no. 5, p. 728 [*Kinet. Catal.* (Engl. Transl.), vol. 47, no. 5, p. 704].
15. Polotebnova, N.A., Nguen Van Cheu, and Kal'nibolotskaya, V.V, *Zh. Neorg. Khim.*, 1973, vol. 18, no. 2, p. 413.
16. Gregg, S.J. and Sing, K.S.W., *Adsorption, Surface Area, and Porosity*, London: Academic, 1967.
17. Fenelonov, V.B., *Vvedenie v fizicheskuyu khimiyu formirovaniya supramolekulyarnoi struktury adsorbentov i katalizatorov* (Introduction to the Physical Chemistry of the Formation of the Supramolecular Structure of Adsorbents and Catalysts), Novosibirsk: Sib. Otd. Ross. Akad. Nauk, 2004.
18. Rocchiccioli-Deltcheff, C., Aouiss, A., Bettahar, M.M., Launay, S., and Fournier, M., *J. Catal.*, 1996, vol. 164, no. 1, p. 16.
19. Yurchenko, E.N. and Detusheva, L.G., *Izv. Sib. Otd. Akad. Nauk SSSR, Ser. Khim.*, 1986, no. 3, p. 51.
20. Bondareva, V.M., Andrushkevich, T.V., Maksimovskaya, R.I., Plyasova, L.M., Ziborov, A.V., Litvak, G.S., and Detusheva, L.G., *Kinet. Katal.*, 1994, vol. 35, no. 1, p. 129.
21. Gayraund, P.-Y., Essayem, N., and Vedrine, J.C., *Catal. Lett.*, 1998, vol. 56, no. 1, p. 35.
22. Okuhara, T., Nishimura, T., Watanabe, H., and Misono, M., *J. Mol. Catal.*, 1992, vol. 74, nos. 1–3, p. 247.
23. Rocchiccioli-Deltcheff, C.R. and Fournier, M., *J. Chem. Soc., Faraday Trans.*, 1991, vol. 87, no. 24, p. 3913.
24. Mizuno, N., Katamura, K., Yoneda, Y., and Misono, M., *J. Catal.*, 1983, vol. 83, p. 384.
25. Maksimov, G.M., Kustova, G.N., Matveev, K.I., and Lazarenko, T.P., *Koord. Khim.*, 1989, vol. 15, no. 6, p. 788.
26. Misono, M., Mizuno, N., and Komaya, T., *Proc. 8th Int. Congr. on Catalysis*, Berlin, 1984, vol. 5, p. V-487.
27. Okuhara, T., Yamada, T., Seki, K., Johkan, K., and Nakato, T., *Microporous Mesoporous Mater.*, 1998, vol. 21, nos. 4–6, p. 637.
28. Barton, T.J., Bull, L.M., Klemperer, W.G., Loy, D.A., McEnaney, B., Misono, M., Monson, P.A., Pez, G., Scherer, G.W., Vartuli, J.C., and Yaghi, O.M., *Chem. Mater.*, 1999, vol. 11, no. 10, p. 2633.